J|A|C|S ARTICLES

Published on Web 06/18/2010

Involvement of the LSPR Spectral Overlap for Energy Transfer between a Dye and Au Nanoparticle

Mani Prabha Singh and Geoffrey F. Strouse*

Florida State University, Department of Chemistry and Biochemistry, Molecular Biophysics Program, Tallahassee, Florida 32306-4390

Received March 16, 2010; E-mail: strouse@chem.fsu.edu

Abstract: Nanometal surface energy transfer (NSET) is a molecular ruler technique that has been utilized to optically probe long distances in biomolecular structures. We investigate the useful spectral range of donor dyes and the importance of overlap between the localized surface plasmon resonance (LSPR) and the donor photoluminescence (520−780 nm) and provide a comprehensive study of the R_0 values for the NSET processes from dyes to 2 nm Au NP (gold nanoparticle). The distance-dependent quenching results provide experimental evidence that the efficiency curve slope, R_0 value, and distance of quenching is best modeled as a surface-mediated NSET process analogous to the predictions of Persson−Lang and Chance−Prock−Silbey (CPS). The results show that the LSPR plays a very important role in the observed quenching of excited-state donors at the surface of the nanometal, and the correlation to the NSET model allows a compilation of the necessary biophysical constants for application within the toolbox of biophysics.

Introduction

During the past decade the development of new donors, acceptors, dark quenchers, and the use of 3-color energy transfer processes has expanded the applicability of optical probe methodologies to a wider range of biological problems.[1−7] Resonant energy transfer methods such as FRET (fluorescence resonance energy transfer),[8,10] LRET (luminescence resonance energy transfer),[9,11] spFRET (single particle FRET),[12,13] NSET (nanometal surface energy transfer),[4,5] BRET (bioluminescence resonance energy transfer),[14] FLIM (fluorescence lifetime imaging),[15,16] as well as others[1] are recognized as important optical tools for probing structural changes in biological systems.

The development of novel acceptors and donors in recent years has focused on the use of metal nanoparticles (NPs) as universal acceptors[20,45,5] and quantum dots (QDs) as tunable donors[7,17−19] due to the unique properties of these materials. QDs can be envisioned as effectively improved dye molecules that can be modeled as classical point dipoles (FRET-like) in an energy transfer assay and offer a tunable donor spectral range.[7,17−19]Metal nanoparticles can act either as a radiative quencher or radiative enhancer, depending on the particle size, shape, composition, and the distance between the donor and metal nanoparticle.[5,20,21,28,31] The competition between enhancement and quenching relates to the magnitude of the electric field at the particle surface and the dielectric dispersion for the materials,[22,26] which give rise to quenching at small sizes and radiative enhancement at larger sizes.[28,31]

The unique properties of metal nanoparticles can be attributed to the absorption and scattering characteristics of the metal nanoparticle, typically referred to as the extinction cross section.[62] The individual scattering and absorption terms relate to the real and imaginary components of the dielectric curve, resulting in the well-known surface plasmon resonance (SPR) at 525 nm in gold nanoparticles. The SPR describes an induced oscillation of electrons in the metal nanoparticle. Changes in the real and imaginary components of the dielectric dispersion curves occur as the metal NP is reduced in size. The change in

(1) Selvin, P. R. *Nat. Struct. Biol.* **2000**, *7*, 730–734.
(2) Ha, T. *Methods* **2001**, *25*, 78–86.
(3) Weiss, S. *Nat. Struct. Biol.* **2000**, *7*, 724–729.
(4) Yun, C. S.; Javier, A.; Jennings, T.; Fisher, M.; Hira, S.; Peterson, S.; Hopkins, B.; Reich, N. O.; Strouse, G. F. *J. Am. Chem. Soc.* **2005**, *127*, 3115–3119.
(5) Jennings, T. L.; Singh, M. P.; Strouse, G. F. *J. Am. Chem. Soc.* **2006**, *128*, 5462–5467.
(6) Jennings, T. L.; Schlatterer, J. C.; Singh, M. P.; Greenbaum, N. L.; Strouse, G. F. *Nano Lett.* **2006**, *6*, 1318–1324.
(7) Medintz, I. L.; Mattoussi, H. *Phys. Chem. Chem. Phys.* **2009**, *11*, 17–45.
(8) Clapp, A. R.; Medintz, I. L.; Mauro, J. M.; Fisher, B. R.; Bawendi, M. G.; Mattoussi, H. *J. Am. Chem. Soc.* **2004**, *126*, 301–310.
(9) Eliseeva, S. V.; Bunzli, J. C. G. *Chem. Soc. Rev.* **2010**, *39*, 189–227.
(10) Stryer, L.; Haugland, R. P. *Proc. Natl. Acad. Sci. U.S.A.* **1967**, *58*, 719–725.
(11) Selvin, P. R.; Hearst, J. E. *Proc. Natl. Acad. Sci. U.S.A.* **1994**, *91*, 10024–10028.
(12) Pons, T.; Medintz, I. L.; Wang, X.; English, D. S.; Mattoussi, H. *J. Am. Chem. Soc.* **2006**, *128*, 15324–15331.
(13) Yasuda, R.; Masaike, T.; Adachi, K.; Noji, H.; Ito, H.; Kinosita, K. *Proc. Natl. Acad. Sci. U.S.A.* **2003**, *100*, 9314–9318.
(14) Pfleger, K. D. G.; Eidne, K. A. *Nat. Methods* **2006**, *3*, 165.
(15) Millington, M.; Grindlay, G. J.; Altenbach, K.; Neely, R. K.; Kolch, W.; Bencima, M.; Read, N. D.; Jones, A.; Dryden, D. T. F.; Magennis, S. W. *Biophys. Chem.* **2007**, *127*, 155–164.
(16) Yasuda, R. *Curr. Opin. Neurobiol.* **2006**, *16*, 551–561.
(17) Fisher, B. R.; Eisler, H. J.; Stott, N. E.; Bawendi, M. G. *J. Phys. Chem. B* **2004**, *108*, 143–148.
(18) Kim, S.; Lim, Y. T.; Soltesz, E. G.; DeGrand, A. M.; Lee, J.; Nakayama, A.; Parker, J. A.; Mihalijevic, T.; Laurence, R. G.; Dor, D. M.; Cohn, L. J.; Bawendi, M. G.; Frangioni, J. V. *Nat. Biotechnol.* **2004**, *22*, 93–97.
(19) Stroh, M.; Zimmer, J. P.; Duda, D. G.; Levchenko, T. S.; Cohen, K. S.; Brown, E. B.; Scadden, D. T.; Torchilin, V. P.; Bawendi, M. G.; Fukumura, D.; Jain, R. K. *Nat. Med.* **2005**, *11*, 678–682.
(20) Pons, T.; Medintz, I. L.; Sapsford, K. E.; Higashiya, S.; Grimes, A. F.; English, D. S.; Mattoussi, H. *Nano Lett.* **2007**, *7*, 3157–3164.
(21) Link, S.; El-Sayed, M. A. *J. Phys. Chem. B* **1999**, *103*, 8410–8426.

the dielectric dispersion results in a broadening of the SPR without a change in the observed SPR energy.[36,37] For ultrasmall metal nanoparticles the SPR will localize at the surface of the gold nanoparticle,[63] resulting in the formation of a localized surface plasmon (LSPR) best described by a skin-depth oscillation of the electric field.

Depending on the nature of coupling between the SPR oscillation and a dye in close proximity to the metal surface, the observation of radiative quenching or enhancement has been empirically described by Lakowicz via the radiating plasmon (RP) model in which quenching arises from the absorption component in the extinction spectra, while the enhancement reflects the scattering contribution.[28] As the nanoparticle is reduced below 40 nm, the absorption term dominates the extinction spectra, and therefore radiative quenching is the predominate component in which energy transfer from the dye to the metal results in electron−hole pair formations (polaritons) and subsequent Ohmic losses. Following from the RP theory, the rate of energy loss will reflect the coherence of the nanoparticle oscillation by influencing the ability of the plasmon to radiate following energy transfer. Increasing the nanoparticle size or changing the shape can lead to larger contributions from the scattering term and therefore enhancement of the dye oscillator rather than quenching.

While substantial effort has been made to look at the enhancement effects, the nature and mathematical understanding of energy transfer quenching of a photoluminescent dye by small gold nanoparticles has received less attention.[32,33] Energy transfer leading to quenching of a dye at or near a small gold nanoparticle surface clearly occurs. However, whether the quenching relates to contributions from the interband transitions or the coupling to the LSPR is unclear.[28] Energy transfer processes must follow the *Fermi Golden Rule* and therefore have constraints with respect to the separation distance, orientation, and energy overlap between the donor and acceptor wave functions.[22,26,27] The spatial orientation terms depend on the description of the donor and acceptor dipole moment and optical properties, while the energy overlap is dependent on the donor photoluminescence (PL) and metal acceptor extinction spectra. When small Au NPs are used as acceptors, the spectral overlap function of interest is between the donor excited state and the frequency of localized surface plasmon resonance (LSPR) for the metal, which can be very broad.[37,63] Chance, Prock, and Silbey solved the *Fermi Golden Rule* problem for the interaction of an energy donor to a metal acceptor. However, in order to treat the energy transfer in a small Au nanometal, the surface-dependent coupling of the donor and the acceptor needs to be described. Persson and Lang derived the energy transfer expression for coupling of the excited-state dipole (donor) to a metal surface (acceptor), predicting that the localization of the electric field oscillation at a thin layer leads to an energy transfer distance dependence that follows R^{-4}, where R is the separation distance between donor and acceptor.[27]

Recent results have shown very efficient quenching of an excited-state dipole near a 2 nm Au NP occurs with a R^{-4} distance dependence via the empirical nanometal surface energy transfer (NSET) mechanism.[4,5] The empirical observation of a R^{-4} distance dependence between a dye and a gold nanoparticle (Au NP) is surprising. In fact, although the results have been experimentally reproduced by a large number of groups,[45−57] quantum mechanical descriptions[44] within the postulates of electrodynamics theory for explaining the quenching mechanism have not reproduced the observed R^{-4} distance dependence. Although the theoretical prediction of Persson and Lang for energy transfer at a thin layer in a bulk material has been extrapolated to explain the observation of quenching of the photoluminescence of QDs[20] and molecular dyes[4,5,30] by 1.5 and 2.0 nm Au NPs, a full theoretical understanding of the process is still required, as the metal NP energy transfer is finding a broad applicability in biophysics,[45−57] and thus a more detailed analysis of quenching across the spectral overlap region for the Au LSPR and compilation of the NSET constants (R_0, range) is needed. A systematic study correlating the overlap of the LSPR spectral range and donor photoluminescence (PL), as well as establishing a set of R_0 constants for NSET, has not

(22) Gersten, J.; Nitzan, A. *J. Chem. Phys.* **1981**, *75*, 1139–1152.
(23) Chance, R. R.; Prock, A.; Silbey, R. *J. Chem. Phys.* **1975**, *62*, 2245–2253.
(24) Kuhn, H. *J. Chem. Phys.* **1970**, *53*, 101–108.
(25) Inacker, O.; Kuhn, H. *Chem. Phys. Lett.* **1974**, *27*, 317–321.
(26) Chance, R. R.; Prock, A.; Silbey, R. *Adv. Chem. Phys.* **1978**, *37*, 1–65.
(27) Persson, B. N. J.; Lang, N. D. *Phys. Rev. B* **1982**, *26*, 5409–5415.
(28) Lakowicz, J. R. *Anal. Biochem.* **2005**, *337*, 171–194.
(29) Jain, P. K.; Lee, K. S.; El-Sayed, I. H.; El-Sayed, M. A. *J. Phys. Chem. B* **2006**, *110*, 7238–7248.
(30) Singh, M. P.; Jennings, T. L.; Strouse, G. F. *J. Phys. Chem. B* **2001**, *113*, 552–558.
(31) Jennings, T.; Strouse, G. *Adv. Exp. Med. Biol.* **2007**, *620*, 34–47.
(32) Dulkeith, E.; Ringler, M.; Klar, T. A.; Feldman, J.; Javier, A. M.; Parak, W. J. *Nano Lett.* **2005**, *5*, 585–589.
(33) Dubertret, B.; Calame, M.; Libchaber, A. J. *Nat. Biotechnol.* **2001**, *19*, 365–370.
(34) Clegg, R. M.; Murchie, A. I. H.; Zechel, A.; Lilley, D. M. J. *Proc. Natl. Acad. Sci. U.S.A.* **1993**, *90*, 2994–2998.
(35) Johnson, P. B.; Christy, R. W. *Phys. Rev. B* **1972**, *6*, 4370–4379.
(36) Kreibig, U.; Vollmer, M. *Optical Properties of Metal Clusters*; Springer-Verlag: New York, 1995; Vol. 25.
(37) Alvarez, M. M.; Khoury, J. T.; Schaaff, T. G.; Shafigullin, M. N.; Vezmar, I.; Whetten, R. L. *J. Phys. Chem. B* **1997**, *101*, 3706–3712.
(38) Wooten, F. *Optical Properties of Solids*; Academic Press, Inc.: New York, 1972.
(39) Hovel, H.; Fritz, S.; Hilger, A.; Kreibig, U. *Phys. Rev. B* **1993**, *48*, 18178–18188.
(40) Turro, N. J. *Modern Molecular Photochemistry*; Benjamin/Cummings: New York, 1978.
(41) Zheng, J.; Zhang, C. W.; Dickson, R. M. *Phys. Rev. Lett.* **2004**, *93*, 077421−077424.
(42) Weare, W. W.; Reed, S. M.; Warner, M. G.; Hutchison, J. E. *J. Am. Chem. Soc.* **2000**, *122*, 12890–12891.
(43) Munoz-Losa, A.; Vukovic, S.; Corni, S.; Mennucci, B. *J. Phys. Chem. C* **2009**, *113*, 16364–16370.
(44) Swathi, R. S.; Sebastian, K. L. *J. Chem. Phys.* **2007**, *126*, 234701(1)−234701(5).
(45) Sen, T.; Sadhu, S.; Patra, A. *App. Phys. Lett.* **2007**, *91*, 043104(1)−043104(3).
(46) Darbha, G. K.; Ray, A.; Ray, P. C. *ACS Nano* **2007**, *2*, 77–84.
(47) Sen, T.; Patra, A. *J. Phys. Chem. C* **2008**, *112*, 3216–3222.
(48) Haldar, K. K.; Patra, A. *Chem. Phys. Lett.* **2008**, *462*, 88–91.
(49) Darbha, G. K.; Lee, E.; Anderson, Y. R.; Fowler, P.; Mitchell, K.; Ray, P. C. *IEEE Sensors J.* **2008**, *8*, 693–700.
(50) Huang, S. X.; Chen, Y. *Nano Lett.* **2008**, *8*, 2829–2833.
(51) Griffin, J.; Ray, P. C. *J. Phys. Chem. B* **2008**, *112*, 11198–11201.
(52) Sen, T.; Haldar, K. K.; Patra, A. *J. Phys. Chem. C* **2008**, *112*, 17945–17951.
(53) Kogot, J. M.; England, H. J.; Strouse, G. F.; Logan, T. M. *J. Am. Chem. Soc.* **2008**, *130*, 16156–16157.
(54) Griffin, J.; Singh, A. K.; Senapati, D.; Rhodes, P.; Mitchell, K.; Robinson, B.; Yu, E.; Ray, P. C. *Chem.−Eur. J.* **2009**, *15*, 342–351.
(55) Chhabra, R.; Sharma, J.; Wang, H. N.; Zou, S. L.; Lin, S.; Yan, H.; Lindsay, S.; Liu, Y. *Nanotechnology* **2009**, *20*, 485201(1)−485201(10).
(56) Kogot, J. M.; Parker, A. M.; Lee, J.; Blaber, M.; Strouse, G. F.; Logan, T. M. *Bioconjugate Chem.* **2009**, *20*, 2106–2113.
(57) Sen, T.; Jana, S.; Koner, S.; Patra, A. *J. Phys. Chem. C* **2010**, *114*, 707–714.
(58) Hagerman, P. J. *Annu. Rev. Biophys. Biol.* **1988**, *17*, 265–286.
(59) Mathew-Fenn, R. S.; Das, R.; Harbury, P. A. B. *Science* **2008**, *322*, 446–449.

appeared. Such a compilation of data will open the applicability of the NSET methods to a wider range of optical applications, and potentially live cell imaging processes.

In this report, we demonstrate a direct correlation between the donor PL energy and the LSPR frequency for a 2 nm Au NP. The 2 nm Au NP is chosen to minimize molecular level contributions for the particle interacting with the DNA spacer, to ensure the LSPR description is appropriate, and eliminate potential contributions from enhancement. In addition, 2 nm Au is selected to better couple to our earlier studies and allow the distance approximations using the Clegg model, since the 2 nm Au is positioned distally.[4,5,30] Analysis of the energy transfer efficiency curves for a wide range of molecular dyes with PL overlapping the LSPR frequency for a 2 nm Au NP (520 nm −720 nm) allows a direct comparison of the experimental results to the theoretical predictions from classical FRET,[10] Gersten−Nitzan (GN),[22] CPS−Kuhn,[24] and NSET[4,5] models for energy transfer between a donor and Au NP. Comparison of the models indicates that the NSET model best describes the observed quenching behavior for a 2 nm Au NP, whereas CPS−Kuhn overpredicts the distance dependence, and FRET and GN under-predict the distance. The agreement of the NSET model may be rationalized if the LSPR oscillation can be approximated by a plane model. The results provide a much needed study to analyze the NSET mechanism for donor−Au NP energy transfer and provide constants for application of NSET as a tool in the biophysics molecular ruler toolbox.

Experimental Section

Au NP−Dye Conjugates. The Au NP−dye conjugates were prepared with the donor dye positioned on a C_6 spacer appended to the 5′-phosphate backbone terminus of a 15bp (base pair), 22bp, 30bp, and 45bp synthetic DNA sequence as described previously.[5,30] The Au−dye separation distance is 68.7, 92.5, 119.7, and 170.7 Å, respectively, based on the Clegg model[34] from the Au NP surface to the center of the donor. Duplex DNA lengths less than 100 nm are assumed to be a rigid rod with only high-frequency oscillations.[58,59] The DNA sequences and list of dyes are included in the Supporting Information (SI1). The Au NP and the dye are positioned at the opposite 5′ ends of the double-stranded DNA via attachment to a C_6-S and $C_6-amine$ at the terminal phosphate, respectively. Stoichiometric exchange is carried out on 2 nm BSPP (bis(sulfonatophenyl)triphenylphosphine) passivated Au NP[5,30] to promote a 1:1 DNA−dye to Au NP ratio via ligand place exchange reactions of the BSPP passivant on the Au NP at a 1:20 mol ratio of Au NP to DNA−dye. The final assemblies were purified by ethanol precipitation and analyzed by polyacrylamide gel electrophoresis (PAGE) to ensure single-site modification and unbound dye removal.

Optical Measurements. Absorption and photoluminescence (PL) experiments were conducted on a Varian Cary 50 UV−vis spectrophotometer and a Varian Cary Eclipse Fluorescence spectrophotometer, respectively, at 293 ± 2 K in 50 μL cuvettes using 200 pmol of double strand DNA (ds-DNA) in 20 mM PBS buffer, 0.1 M NaCl, pH 7.5. Excited-state PL lifetime measurements were carried out at $\lambda_{ex} = 290$ nm (≤1 mW power) by frequency doubling the output of a R6G dye laser (Coherent 702-1), $\lambda = 590$ nm pumped by $NdVO_4$ laser (Spectra-Physics Vanguard, 2 W, 532 nm, 76 MHz, 10 ps) for AF488. The direct output of the R6G dye laser of $\lambda_{ex} = 560$ nm (<1 mW) was used for AF555, $\lambda_{ex} = 590$ nm for AF594 and $\lambda_{ex} = 620$ nm (<1 mW) for AF647, AF700, and AF750. The output of the dye laser was cavity dumped at 1.9 MHz to optimize collection. The PL of the dye under excitation was directed to a Chromex 500 is 0.5 m imaging monochromator at right angles which is focused into a Hamamatsu C5680 streak camera operating at a 10 ns window or 20 ns window, depending on the native lifetime of the dye under observation. The experimental data represent 800,000 collection events. The lifetimes were fit to a single exponential function ($I(t) = A \exp(-kt + c)$) using a linear least-squares fitting routine.

The quenching efficiency (E) at a particular donor−acceptor (D−A) separation distance is calculated by measuring the emission intensity (I') and/or the lifetime (τ') of the dye with the Au NP appended to the ds-DNA (referred to as the *sample*) relative to the intensity (I_0) and/or lifetime (τ_0) of the dye coupled to duplex DNA when the Au NP is not appended at the complementary 5′ end (referred to as the *control*). Comparisons to the lifetime of the dye on a single-strand DNA to the double strand DNA sequence allows correction for any dye−DNA interactions affecting the observed Φ_{em} or τ.[40] It is to be noted that DNA sequences are identical for each defined dye−Au NP separation distance regardless of the dye used.

Results

Experimental Results for the Dye to Metal NP Energy Transfer. The distance dependence for energy transfer from a donor to a 2 nm Au NP was measured for a range of molecular dyes with PL between 520 and 780 nm. As shown schematically in Figure 1a, the separation distance is controlled by using a duplex DNA spacer (3.4 Å per base pair) in which the Au NP and dye are appended at complementary 5′ ends through a C_6 spacer attached to the phosphate backbone.Using the Clegg model,[34] the distance of separation was defined as the center of the dye to the surface of the Au NP for all energy transfer models. Contributions from the spacer is included for the C_6 spacer as described previously for both the dye and the Au NP.[5,30] the experimental sequences and separation distances are presented in the Supporting Information (S1).

The dye PL spectra and the extinction spectrum for 2 nm BSPP passivated Au are shown in Figure 1b. The Au extinction spectra includes contributions from the LSPR, the interband transitions, and ligand absorptions at >350 nm. The dashed line in Figure 1b represents the LSPR contribution calcualted by fitting the extinction spectra for a 2 nm Au NP using Mie theory and subtracting the ligand absorption and higher-order interband contributions to the extinction spectra (Supporting Information S2). For a spherical Au NP, the extinction spectra can be interpreted by classical electrodynamics if we treat the Au nanoparticle as a Fermi gas or within the Drude approximation by inclusion of the overlapping interband transitions (d → p).[36] The interband transitions are assumed to be invariant with size, while the Drude contribution is size dependent.[36,37] For a spherical Au NP, the electron-scattering term A is assumed to be isotropic and is fixed to a value of 1.0.[36,37] Although changes in the value of A can lead to damping and frequency shifts in the LSPR, the spectra in Figure 1b can be adequately interpreted using $A = 1$ (*Supporting Information* S3).[37] The steady-state photoluminescence (PL) and lifetime (τ) quenching data for the donors as a function of the distance of separation from the 2 nm Au NP are shown in Figure 2 and summarized in Table 1. Inspection of the data shows a clear distance dependence for excited-state quenching for all measured dyes when the PL overlaps with the Au NP LSPR band. No quenching is observed for AF750, which lies outside the spectral region for the 2 nm Au NP LSPR. In the experiment, quenching data on AF594 and AF647 are shown at a single distance. The correlation between the observed fluorophore quenching and the energy of the discrete LSPR extinction features suggests that energy transfer from a point dipole to a Au NP surface occurs only within the limit of the LSPR frequency.

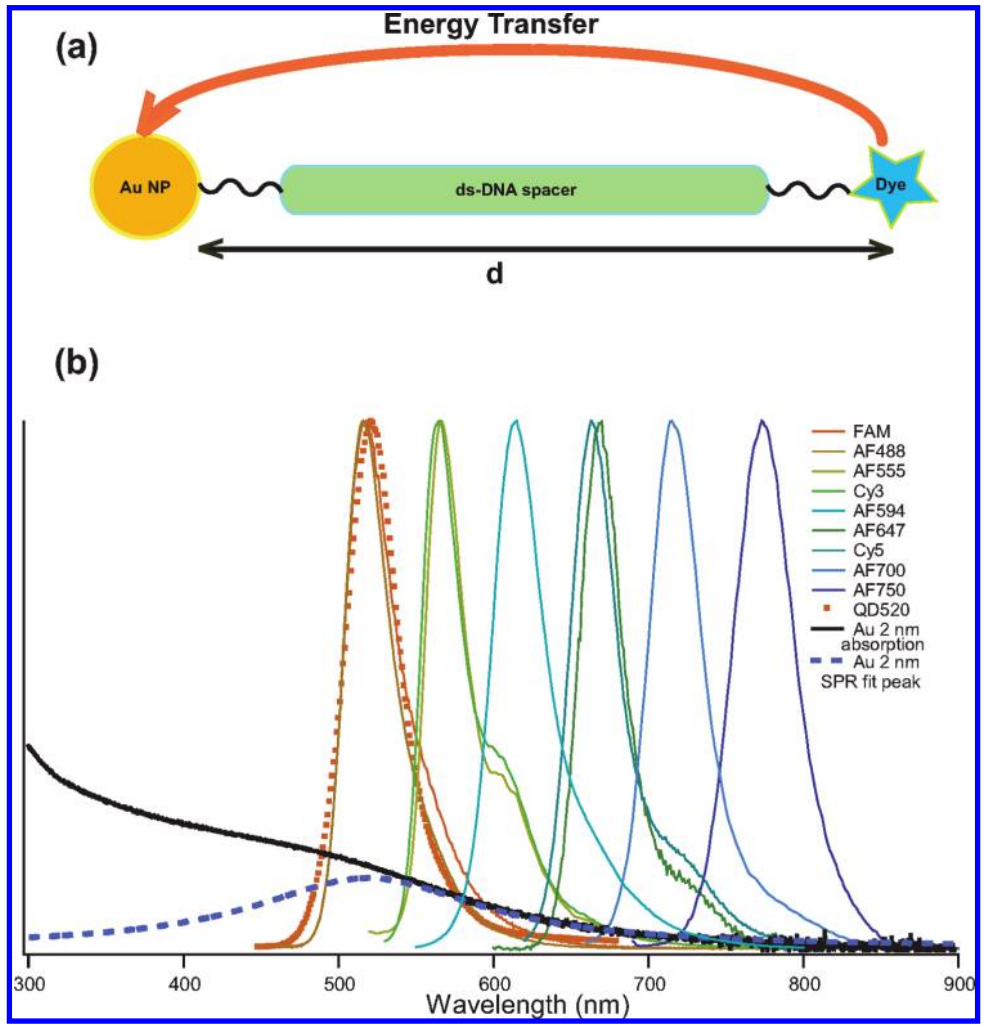

Figure 1. (a) Energy transfer schematic showing the assembly of DNA with a 2 nm Au NP appended at one end and a photoluminescent dye at the complementary end. (b) Normalized PL spectra of the donors and the extinction of BSPP-coated, water-soluble 2 nm Au nanoparticles. The dashed line represents the calculated LSPR for a 2 nm Au NP.

Theoretical Considerations and Comparison to Experimental Data. In a Au NP, the effect of the change in dielectric dispersion with size has several effects on the properties of the Au NP. In a 2 nm spherical nanoparticle the transverse and longitudinal plasmons lie at identical energies and more importantly, the absorptive cross section dominates the extinction spectra. In addition, due to the size-dependent change in dielectric constants, at 2 nm the scattering contribution is negligible and therefore enhancement should not play a significant role in the excited decay process for a dye near a metal nanoparticle. This implies that radiative quenching due to the absorptive component of the extinction cross-section will dominate the energy relaxation pathway for an excited-state dye close to a metal nanoparticle surface.[28,29,32] Several energy transfer theories can be used to account for the observed quenching of the photoluminescent donor by the metal nanoparticle, including FRET,[1,8,10] NSET,[4−6,45−57] GN,[22,32] DMPET (dipole to metal particle energy transfer)[20] and CPS−Kuhn[24−26] models. Each model has a set of limitations imposed upon it to account for changes in the dielectric properties as the metal is reduced in dimension.

To fully interrogate the energy transfer quenching mechanism between a dye and a 2 nm Au nanoparticle, the properties of Au in the 2 nm size regime must be considered. For sizes approaching molecular clusters,[36,41] the metal is expected to lose its metallic properties, lose its ideal mirror behavior, localize the electron density at the surface of the NP and may be expected to behave as a single point dipole.[41,43] Ideal mirror behavior depends on the metal's optical properties *viz* its complex refractive index, $n = n_r + ik$ and the dielectric function, $\varepsilon = \varepsilon_1 + i\varepsilon_2$. For a bulk metal, the perfect mirror behavior breaks down at frequencies close to the plasma frequency ω_p where the real part of the dielectric constant, ε_1 becomes positive and large and the imaginary component of the refractive index, k approaches zero. For very small clusters the ideal mirror behavior breaks down due to the size dependent expression for the dielectric function.[36] This is seen by solving the Kreibig expression for a 2 nm Au NP (Supporting Information Figure S2) where a very large value of ε_1 and a near zero value of k results in the loss of the metal reflectivity[36,38] and the breakdown of an ideal mirror assumption. It should be noted that the breakdown of the ideal mirror assumption does not imply loss of metallic behavior (i.e., Ohmic loss, polariton formation and strong dipole coupling within the metal).[41,43] Therefore, at small Au NP sizes the change in dielectric function will impact the nature of energy transfer between a Au NP and a dye.

The simplest mechanism to describe resonant energy transfer is Forster resonance energy transfer (FRET). FRET is a molecular level approximation treating the donor and acceptor as zero-dimensional resonantly coupled oscillators operating

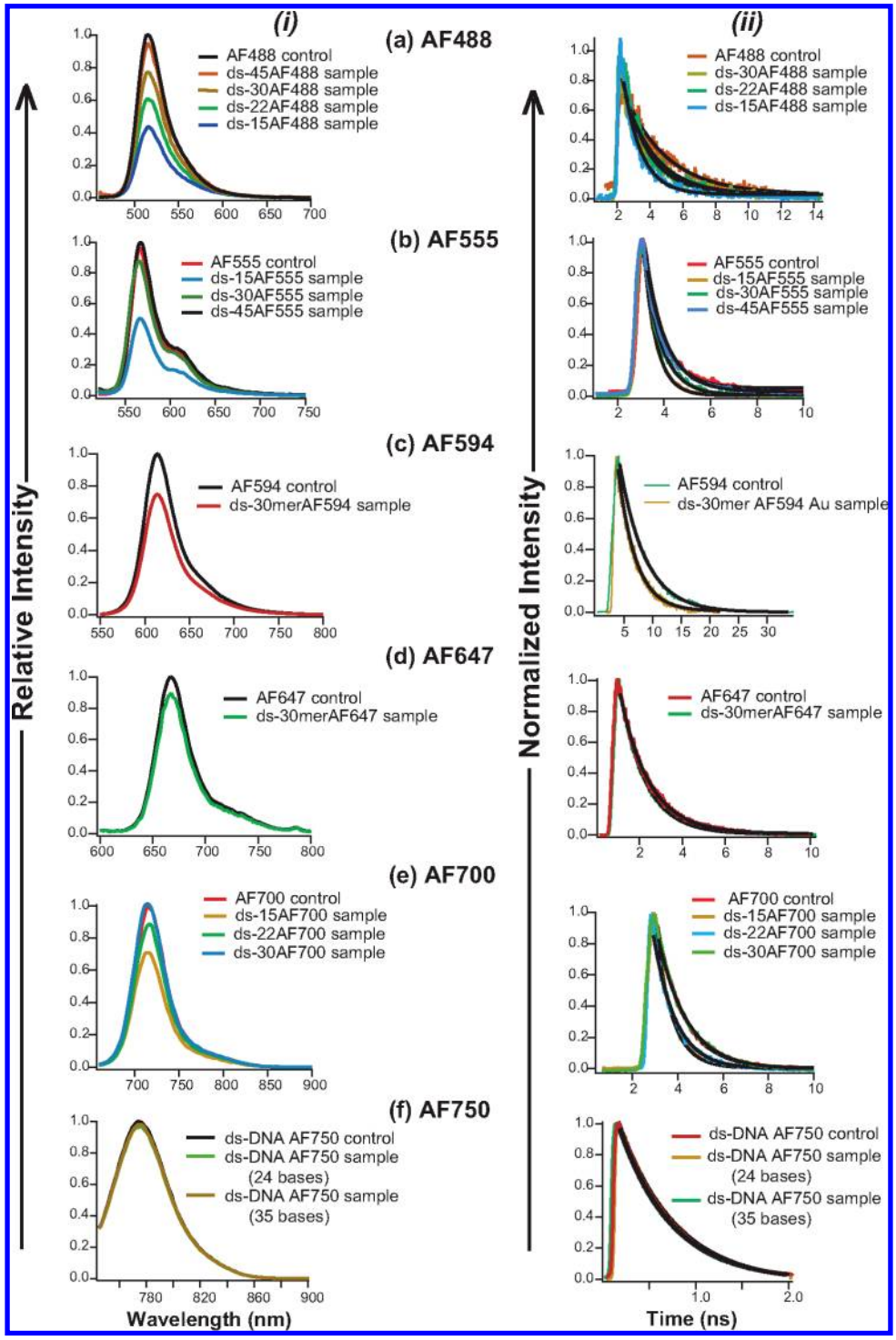

Figure 2. Distance-dependent quenching of donor dyes by (*i*) PL intensity and (*ii*) lifetime analysis for (a) AF488, (b) AF555, (c) AF594, (d) AF647, (e) AF700, and (f) AF750.

within the limit of weak coupling over distances in excess of the length of the dipole.[10] For Au NPs, the FRET approximation assumes the Au NP is molecular and no perturbation of the donor occurs by the Au NP. In the theory proposed by Gersten−Nitzan (GN), the Au NP has a strong electric field, and the response of a single-point dipole (donor) placed close to a metal nanoparticle is reflected in changes in the radiative and nonradiative rates of decay due to coupling of the donor to the metal's local electric field.[22] NSET assumes coupling between a point dipole and applies a thin film approximation to describe the two-dimensional LSPR at the surface of the metal NP. In NSET, the metal oscillators are considered to be strongly coupled[27] as predicted by the Drude model, rather than a collection of independent oscillating dipoles or a single dipole in analogy to the FRET model. In CPS−Kuhn the dye molecule is treated as a classical linear harmonic oscillator which casts an image dipole onto the metal surface. The CPS−Kuhn model assumes the metal to be a perfect mirror in order to account for the behavior of a point dipole near the metal surface.[24,26] The coupling of the donor dipole to the metal, which is described

Table 1. Experimentally Observed Distance-Dependent Quenching in Normalized PL (I'/I_0) and Lifetime τ' for AF488, AF555, AF594, AF647, AF700, and AF750; PL Wavelength (λ_{em}) and the Natural Lifetime (τ_0) for Each Dye Is Listed

dye	base pairs	distance (Å)	I'/I_0	τ' (ns)
AF488	15	68.75	0.41	1.12 ± 0.2
$\tau_0 = 2.6 \pm 0.03$ ns	22	93.08	0.57	1.56 ± 0.03
$\lambda_{em} = 519$ nm	30	118.1	0.73	2.00 ± 0.02
	45	170.0	0.95	2.39 ± 0.01
AF555	15	68.75	0.46	0.53 ± 0.02
$\tau_0 = 0.94 \pm 0.01$ ns	30	118.1	0.90	0.80 ± 0.01
$\lambda_{em} = 565$ nm	45	170.0	0.99	0.89 ± 0.2
AF594				
$\tau_0 = 4.45 \pm 0.02$ ns	30	118.1	0.75	3.07 ± 0.02
$\lambda_{em} = 612$ nm				
AF647				
$\tau_0 = 1.36 \pm 0.01$ ns	30	118.1	0.88	1.19 ± 0.02
$\lambda_{em} = 668$ nm				
AF700	15	68.75	0.70	0.70 ± 0.02
$\tau_0 = 1.1 \pm 0.02$ ns	22	93.08	0.90	0.97 ± 0.01
$\lambda_{em} = 719$ nm	30	118.1	0.99	1.1 ± 0.01
	45	170.0	0.99	1.1 ± 0.02
AF750	24	77.3	0.95	0.56 ± 0.02
$\tau_0 = 0.61 \pm 0.01$ ns	35	94.3	0.93	0.58 ± 0.01
$\lambda_{em} = 780$ nm				

by treating the metal NP as an ideal mirror, leads to the potential for both enhancement and quenching, depending on the projection of the electric field from the NP surface, which will be size dependent.[28,36,39] DMPET is a combination of FRET and NSET, and experimental results on a 2 nm Au NP indicates the NSET component dominates the experimental observation[20] and therefore is not discussed further as a separate theory. Although all these mechanisms can be used to approximate the energy transfer efficiency, each mechanism exhibits a limitation with respect to the accuracy of the fit.

For comparison of theory to experiment three terms will be important to extract the 50% quenching distance R_0, the power law (n) for quenching efficiency (E) and the total quenching range (10−90% quenching efficiency) for each theory. FRET, NSET, GN, and CPS−Kuhn mechanisms will have distinct distances over which they operate, size regimes for the metal that would be applicable, and constraints with respect to the nature of the dipoles involved.

The R_0 values for a specific dye−metal pair can be calculated for each theory. The R_0^{FRET} is[10]

$$R_0^{FRET} = \left[\frac{9000(\ln 10)\kappa^2\Phi_{dye}}{128\pi^5 N_A n^4} J(\lambda)\right]^{1/6} \quad (1)$$

where κ is the orientation factor, Φ_{dye} is the quantum yield of the donor, N_A is the Avogadro's number, n is the refractive index of the medium, and $J(\lambda)$ is the overlap integral between the donor emission and the acceptor absorption.

The value R_0^{GN} for a small metal nanoparticle can be expressed in terms of[22]

$$R_0^{GN} = \left[2.25 \cdot \frac{c^3}{\omega_{dye}^3} \cdot \Phi_{dye} \cdot a^3 \cdot \frac{(\varepsilon_1 + 2)^2 + \varepsilon_2^2}{\varepsilon_2}\right]^{1/6} \quad (2)$$

where, ω_{dye} is the frequency of the donor dye, Φ_{dye} is the quantum yield of the donor, a is the radius of the metal nanoparticle, ε_1 and ε_2 are the real and imaginary components of the dielectric constant of the metal,respectively, and c is the speed of light. Equation 2is derived under the assumptions that there is no change in the radiative rate of the dye molecule in the presence of the metal NP and therefore no enhancement effects.

The $R_0^{CPS-Kuhn}$ for the CPS−Kuhn model is described as,[24−26]

$$R_0^{CPS-Kuhn} = \frac{\alpha\lambda}{n}(Aq)^{1/4}\left[\frac{n_r}{2n}\left(1 + \frac{\varepsilon_1^2}{|\varepsilon_2|^2}\right)\right]^{1/4} \quad (3)$$

where A is the absorptivity of the mirror. $A = (4\pi k d_2)/(\lambda)$, and $\alpha = ((1)/(4\pi))(9)^{1/4}$ for a dipole oriented perpendicularly to the metal surface, while it takes a value of $((1)/(4\pi))((9)/(2))^{1/4}$ when the dipole is aligned parallel to the metal surface. λ is the emission wavelength of the donor dipole; ε_1, ε_2, and n_r, k are the real and imaginary components of the dielectric constant and the refractive index of the metal, respectively; n is the refractive index of the medium, and d_2 is the thickness of the mirror, which in this case will be the diameter of the metal nanoparticle. In CPS−Kuhn, it is assumed that the dielectric constants are not size dependent. However, as shown by Kreibig,[36] a modification to the CPS−Kuhn theory incorporating the size dependence of the dielectric constants can be accounted for by substituting a size-dependent term for the dielectric constants.[36,38,39]

The theoretical value for the NSET R_0^{NSET} value is calculated using the NSET expression,[5,23,26,27]

$$d_0^{NSET} = \left(0.225 \cdot \frac{\Phi_0}{\omega_{dye}^2} \cdot \frac{1}{\omega_F k_F} \cdot c^3\right)^{1/4} \quad (4)$$

where, $k_F = 1.2 \times 10^8$ cm^{-1} and $\omega_F = 8.4 \times 10^{15}$ rad/s are the constants for the metal acceptor derived from bulk gold; ω_{dye} and ϕ_{dye} represent the angular frequency of donor emission, and the quantum yield of the donor, respectively, and $c = 3.0 \times 10^8$ m/s is the speed of light.

The efficiency of quenching (E) for steady-state PL quenching can be related to the intensity efficiency, $E(I)$

$$E(I) = 1 - \left(\frac{I'}{I_0}\right) \quad (5)$$

or to the efficiency for quenching of the excited-state donor lifetime $E(\tau)$, and this relationship can be written as

$$E(\tau) = 1 - \left(\frac{\tau'}{\tau_0}\right) \quad (6)$$

A generic form of the efficiency of quenching allows the distance of separation between the donor and acceptor (R) and the R_0 value to be solved, leading to a power law distance dependence where

$$E = \frac{1}{1 + (R/R_0)^n} \quad (7)$$

and the exponent n is dependent on the nature of energy transfer. The FRET and GN models predict an $n = 6$ distance-dependent quenching efficiency, while NSET and CPS−Kuhn are expected to follow an $n = 4$ distance dependence. Solving the efficiency

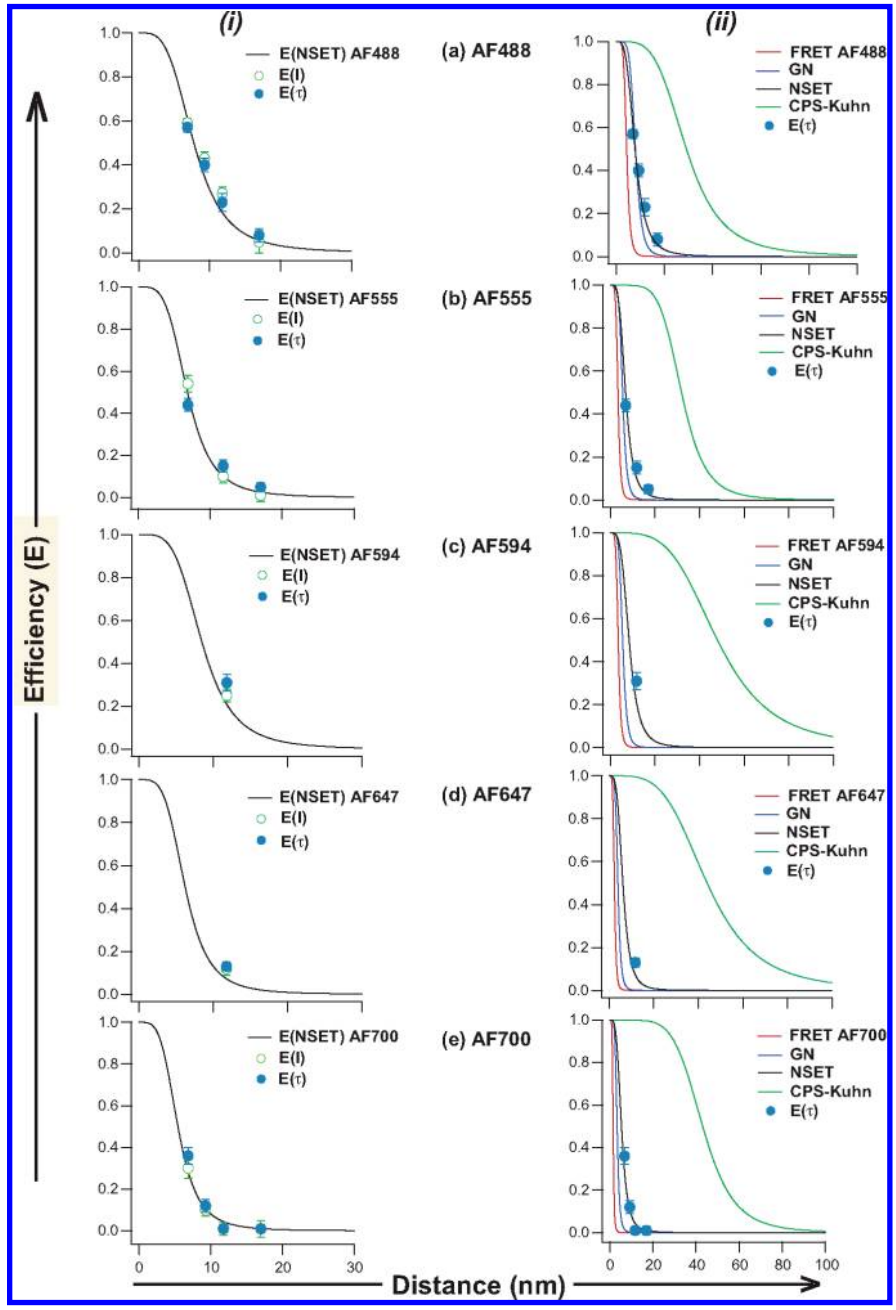

Figure 3. (*i*) Efficiency curve fit of experimental PL and τ data for (a) AF488, (b) AF555, (c) AF594, (d) AF647, and (e) AF700. (*ii*) Comparing the theoretical plots for three energy transfer mechanisms FRET, GN, NSET, and CPS−Kuhn models for (a) AF488, (b) AF555, (c) AF594, (d) AF647, and (e) AF700. The plots were generated with the quantum yield of the dyes as mentioned in Table 1. The constants for the metal to be used in the CPS−Kuhn model were taken from the values published by Johnson and Christy.[35]

and R_0 values with respect to the distance predicts the range of quenching will be greatest for CPS−Kuhn and smallest for FRET.

An empirical fit to eq 7 of the experimental intensity and lifetime quenching data (E^I_{NSET}, E^τ_{NSET}) vs distance is presented in Figure 3(*i*) for each dye−Au NP pair. The plotted E curve in Figure 3(*i*) represents the lifetime quenching data, which is believed to be more accurate as compared to intensity quenching data due to the ability to discriminate subtle changes in lifetime and eliminate unbound dye contributions. The average value observed for all donors that exhibit quenching yields an approximate value of $n = 4$, with experimental values of 3.6, 4.00, and 4.00 for AF488, AF555, and AF700, respectively. The value of $n \approx 4$ was observed previously for FAM ($n =$ 4.0), Cy3 ($n = 3.9$), and Cy5 ($n = 3.8$). In Table 2, the values for each of the dyes, their quantum yield (Φ_{dye}), lifetimes (τ_0), angular frequencies (ω_{dye}), and the theoretical R_0 from the NSET theory are tabulated. Only single-point distance measurements were carried out for AF647 and AF594 by lifetime analysis, and therefore, the R_0 values are calculated in the table by assuming $n = 4$ for efficiency curve. Results for the fluorophores (FAM, Cy3, Cy5, QD520)[5,6,20,30] are not shown in Figure 2 but are included in Table 2 based on previously reported results.

The results of the distance-dependent lifetime quenching assay can be compared to the theoretical plots (Figure 3 (*ii*), Supporting Information S5) generated from the established FRET, GN, NSET, and CPS−Kuhn models by solving eqs 1−4. Comparison of the slope, R_0 values, and distance over which

Table 2. NSET and Dye Constants for Donors to 2 nm Au NP Energy Transfer

dye	λ_{em} nm	ω_{dye} s^{-1}	Φ_{dye}	τ_0 ns	R_0 ($n = 4$) Å
FAM[5,30]	520	3.63×10^{15}	0.9	3.1	80.2
AF488	519	3.63×10^{15}	0.8	2.6	77.9
AF555	565	3.33×10^{15}	0.4	0.9	68.2
Cy3[6]	570	3.31×10^{15}	0.2	1.9	57.6
AF594	612	3.08×10^{15}	0.8	4.5	84.5
Cy5[5,30]	670	2.81×10^{15}	0.25	1.4	66.1
AF647[6]	668	2.82×10^{15}	0.2	1.5	62.4
AF700	719	2.61×10^{15}	0.1	1.1	54.6
AF750	775	2.43×10^{15}	0.1	0.4	–
QD520[20]	520	3.63×10^{15}	0.2	–	55.1

quenching occurs to the theoretically predicted efficiency (E) curves for FRET, GN, NSET, and CPS−Kuhn show that the best experimental fit for the data is to the NSET model for all dyes that exhibit quenching. The FRET and GN models generally fail to predict slope, R_0, and range for the reported dyes. The CPS−Kuhn overpredicts R_0 and range but accurately predicts the slope. Only NSET is able to fit slope and predict accurate R_0 values as well as the quenching efficiency range.

While the theoretical agreement is strongly supportive of the NSET model, an alternate explanation for the failure of the models to describe the experimental observation that must be discounted is the propensity for DNA to interact with the Au NP surface, which would modulate the actual experimental distance. DNA with length scales below 100 nm is generally considered to follow a rigid rod approximation for energy transfer studies;[58,59] however, DNA interaction with large gold particles has been reported.[60,61] Such molecular-level interactions with the large surface area on a Au NP may give rise to an identifiable shift in the LSPR band extinction spectra that correlates with the number and type of molecular interactions present.[63] In addition, changes in the damping constant (A) in eq 1 could also arise if electron scattering is influenced by the DNA binding event. No shift in the experimental spectra is observed upon binding of the DNA to the 2 nm Au nanoparticle (Supporting Information Figure S4). The lack of a LSPR shift for the 2 nm Au nanoparticles is not conclusive evidence, however, as it has been reported that the magnitude of shift is small for Au nanoparticles below 4 nm.[63]

The 2 nm Au NP in this study was designed to minimize nonspecific interactions through the passivation of the surface with the negatively charged (2^-) ligand BSPP in order to increase electrostatic repulsion between the DNA phosphate backbone and the Au NP surface. Earlier studies have shown the use of BSPP is an effective approach to position the 2 nm Au NP distally on the DNA.[64] Although interactions can still arise via van der Waals forces or interactions between the phosphate groups on the DNA and the Au NP surface, it is believed the nonspecific interactions are not contributing to the experimental observations. If an interaction with the Au NP surface was strong, then the predicted perturbation to the efficiency curve would be an offset to the distance and not necessarily a change in the slope of the efficiency curve. Alternatively, if we consider the surface curvature for the 2 nm Au NP and include a 1 nm spacer for the BSPP ligand, then the length of DNA to wrap around a hemisphere is readily calculated as $l = \pi r$, for a BSPP passivated 2 nm Au nanometal $l = 6.28$ nm. A strong interaction of DNA with the Au nanometal would therefore result in approximately 15bp interacting with the Au surface and a reduction in the distances calculated from the Clegg model of ~12 nm. The distance is far too extreme for the longest DNA lengths to be accommodated. The presumption of weak Au NP−DNA interactions being the culprit for failure of the models is further supported by our observation that the NSET model is valid whether the dye modification is terminally[5] or internally independent of salt concentration,[30] and the experimental agreement observed between optically measured RNA hammerhead structures and crystallographically determined distances when using a sub 2 nm Au NP NSET assay.[6] While it is still possible that a variable degree of interaction with the double strand may reduce this distance offset and produce an apparent slope change, we believe that Au−DNA interactions are minimal due to the size of the Au and negative charge of the passivated Au NP; thus, the model failures are unlikely to arise from nonspecific interactions. Thus, the failure of the models to predict both the observed slope and R_0 values across the whole spectral range must reflect the limits imposed on the mechanism to solve the Fermi Golden rule for these models, which do not adequately describe the coupling between a point dipole and a small metal NP.

Conclusion

Physically, it is not appropriate to define the 2 nm Au NP within the limits of the Persson−Lang surface energy transfer (SET) model, which requires the interface to be represented as an infinite plane of which a spherical metal particle is not. The strong correlation between the experimental measurements and the theoretical fits however suggest the Persson−Lang model adequately predicts the NSET observation. The correlation of theory and experiment may suggest that, in general, a metal nanoparticle of a few nanometers in size can be described as a collection of strongly coupled surface-localized dipoles that approach a hemispherical approximation of a plane, which would be consistent with the description for the LSPR in gold where the surface of a Au NP consists of a localization of the electron density at skin depth of the nanoparticle.[63] In order to fully integrate the theory and experiment, further understanding of the changes in the quenching properties with Au NP size, and the importance of the admixture of the d → p interband transitions needs to be interrogated. Regardless, it is clear a correlation exists between the magnitude of quenching and the spectral overlap for the Au nanoparticle LSPR and the dye photoluminescence energy.

The FRET and CPS−Kuhn models clearly fail to fit the experimental data, while the GN model only adequately fits AF488 but fails as the dye PL wavelength is shifted toward the lower energy of the LSPR. The correlation between the NSET model predictions and the experimental results strongly supports the Persson−Lang model as a basis for describing the energy transfer from the donor to the metal surface of the 2 nm Au NP. The correlation may only be applicable to metal nanoparticles where the absorption cross section dominates the extinction spectra and is expected to fail as the Au nanoparticle size is increased due to increasing contributions from the scattering

(60) Brewer, S. H.; Glomm, W. R.; Johnson, M. C.; Knag, M. K.; Franzen, S. *Langmuir* **2005**, *21*, 9303–9307.
(61) Asuri, P.; Bale, S. S.; Karajanagi, S. S.; Kane, R. S. *Curr. Opin. Biotechnol.* **2006**, *17*, 562–568.
(62) Drexhage, K. H. *J. Lumin.* **1970**, *1.2*, 693–701.
(63) Jensen, T.; Kelly, L.; Lazarides, A.; Schatz, G. C. *J. Cluster Sci.* **1999**, *10*, 295–317.
(64) Yun, C. S.; Khitrov, G. A.; Vergona, D. E.; Reich, N. O.; Strouse, G. F. *J. Am. Chem. Soc.* **2002**, *124*, 7644–7645.

cross section.[65] Comparison of the experimental and theoretical results delineates the applicability of different mechanisms to the experimental system under study and the limitations imposed. FRET assumes a point dipole for both donor and acceptor, which does not adequately describe the strongly coupled limit for dipoles in a Au NP. The limit imposed on the Gersten−Nitzan theory considers enhancement effects that can take place at the surface of a larger metal nanoparticle, where the electric field extends off the surface; thus, the failure of the GN model can be attributed to the rapid damping experienced for the electric field at the surface of a 2 nm Au NP. The failure of the CPS−Kuhn model can be attributed to the primary assumption that the Au NP can be treated as a perfect mirror.

The results of this study provide a detailed compilation of experimentally determined R_0 values for dyes that overlap with the 2 nm LSPR band, providing a powerful collection of constants for application of NSET in biophysical studies. Although a theoretical basis from the first principles has not been solved, it is clear that the CPS−Persson model coupled to the LSPR frequency restriction inherent in NSET, predicts the R^{-4} distance dependence observed for all dyes within the LSPR frequency. Further studies are underway to mathematically correlate the empirical observation of NSET with the theoretical predictions for energy transfer at small Au NP surfaces.

Acknowledgment. We thank the National Institute of Health for financial support under Grant No. NIH-GM-079592.

Supporting Information Available: Sequence used for the experiments, AF750 data, effect of the size of the metal NP on the shape LSPR and a comparison of the FRET, GN, and NSET models. This material is available free of charge via the Internet at http://pubs.acs.org.

JA1022128

(65) Singh, M. P. Strouse, G. F. Unpublished results.